



VX-765 ameliorates renal injury and fibrosis in diabetes by regulating caspase-1-mediated pyroptosis and inflammation

Si Wen^{1,2} , Fei Deng³, Lulu Li¹, Li Xu^{1,4} , Xin Li¹, Qiuling Fan^{1*}

¹Department of Nephrology, First Hospital of China Medical University, Shenyang, China, ²Department of Nephrology, First Affiliated Hospital of Dalian Medical University, Dalian, China, ³Department of Urology, Second Xiangya Hospital of Central South University, Changsha, China, and ⁴Department of Laboratory Medicine, First Hospital of China Medical University, Shenyang, China

Keywords

Caspase-1, Diabetic nephropathy, GSDMD, Inflammation, Pyroptosis, VX-765

*Correspondence

Qiuling Fan
Tel.: 86 13904012680
Fax: 86-13904012680
E-mail address:
cmufql@163.com

J Diabetes Investig 2022; 13: 22–33

doi: 10.1111/jdi.13660

ABSTRACT

Introduction: As a lytic inflammatory cell death, pyroptosis has been recently described but has not been unequivocally elucidated in diabetic nephropathy (DN). VX-765 is a safe and effective inhibitor of caspase-1, that was well tolerated in a phase II clinical trial in patients with epilepsy, but its application in DN is still undefined.

Materials and Methods: Immunoblot, co-immunoprecipitation, confocal microscope and flow cytometry were used to analyze the effects of glucose on pyroptosis in renal tubular epithelia (HK-2). *In vitro*, selective caspase-1 inhibitors VX-765 and Z-YVAD-FMK were administered. Pyroptosis and fibrogenesis were determined by immunoblot, ELISA, cytotoxicity assay and flow cytometry. *In vivo*, diabetic mice were administered with 100 mg/kg VX-765. Renal function, pathological changes, and the expressions of NLRC4, GSDMD, IL-1 β , collagen I, fibronectin and CD45 in renal cortex were evaluated.

Results: We identified NLRC4 as a sensor for caspase-1 activation. Moreover, we provided morphological and molecular evidence for pyroptosis in glucose-stressed tubular cells, including ballooned cell membrane, caspase-1 immunoreactivity, GSDMD cleavage, and the release of inflammatory cytokine and cellular contents. All these effects were prevented by treatment with VX-765 or Z-YVAD-FMK, confirming that caspase-1 effectively regulates the occurrence of pyroptosis in HK-2 cells. *In vivo*, treatment of diabetic animals with VX-765 ameliorated renal function, suppressed inflammatory cell infiltration and pyroptosis-associated protein expression, and mitigated tubulointerstitial fibrosis.

Conclusions: This work revealed that caspase-1-mediated pyroptosis drives renal inflammation and fibrosis in diabetes. Our results are the first demonstration of VX-765 representing a promising therapeutic opportunity for alleviating the progression of DN.

INTRODUCTION

Diabetic nephropathy (DN) is the common complication of diabetes and leading cause of end-stage renal disease. The current therapies, including strict blood pressure and glycemic control, cannot effectively delay or prevent the progress of DN. Therefore, exploring new therapeutic strategies is the scientific problem that needs to be solved. The current view of DN has been mainly focused on glomeruli. While clearly of great importance, glomeruli injury is not the primary determinant of renal prognosis in diabetes¹. In diabetic nephropathy, tubular injury correlates

more closely with renal dysfunction than glomerular damage². In recent decades, tubulointerstitial lesion has emerged as an important feature of DN, and is conceived of certain independent value, which occurs even earlier than glomerular lesion.

The state of microinflammation has been perceived as the critical mechanism in the occurrence and development of DN³. Inflammasome activation has recently been reported in multiple renal resident cells and demonstrated in diabetic nephropathy^{4,5}. Pyroptosis is an inflammatory form of programmed cell death driven by inflammatory caspase-1, caspase-4, and caspase-5 in humans (caspase-1 and caspase-11 in mice) following infection or cellular damage⁶. Pyroptosis is a process of cell swelling and rupture that is driven by gasdermin D (GSDMD)-mediated pore

Received 10 May 2021; revised 23 August 2021; accepted 1 September 2021

formation. Upon cleavage by proinflammatory caspases at Asp275, the N-terminal p30 fragment of GSDMD is released and forms pores in the plasma membrane^{7,8}. Of these caspases, caspase-1 is regarded as the strongest executor of GSDMD cleavage⁹. As an innate immune response, pyroptosis is thought to be restricted to immune cells. Whether renal resident cells promote diabetic nephropathy by pyroptosis and how pyroptosis of these cells might be controlled remain elusive.

VX-765 is a potent bioavailable and nontoxic small molecule inhibitor of caspase-1¹⁰. VX-765 has been proved to be safe for humans by oral administration in a 6-week-long phase II clinical trial that studied epilepsy^{11,12}. Therefore, VX-765 is a feasible drug that could rapidly be tested in patients with diabetic nephropathy. Previous studies have demonstrated that caspase-1-deficient diabetic mice are protected against albuminuria and glomerular extracellular matrix accumulation^{4,13}. However, whether caspase-1 manipulation exerts renoprotective effects on DN by regulating pyroptosis is still unknown, and the application of VX-765 in DN is still undefined.

We hypothesized that caspase-1-mediated pyroptosis occurs in the renal tubular epithelium, and that VX-765, a clinical-grade drug, is a previously unrecognized therapeutic approach for mitigating the progression of DN.

MATERIALS AND METHODS

Antibodies and reagents

Anti-GSDMD (Cat. no. NBP2-33422), anti-NLRC4 (Cat. no. NB100-56142), anti-CD45 (Cat. no. NB100-77417) and anti-fibronectin (Cat. no. NBP1-91258) were obtained from Novus (Centennial, CO, USA). The anti-caspase-1 polyclonal antibody (Cat. no. ab1872) was obtained from Abcam (Cambridge, MA, USA). Anti-IL-1 β (Cat. no. 12242) and anti-caspase-5 (Cat. no. 46680) were obtained from Cell Signaling Technology (Danvers, MA, USA). Anti-caspase-4 (Cat. no. 11856-1-AP), anti-collagen type I (Cat. no. 14695-1-AP) and anti- β -actin (Cat. no. 60008-1-Ig) were obtained from Proteintech (Wuhan, China). Alexa Fluor 488-conjugated secondary antibody (Cat. no. ab150089) was obtained from Abcam. VX-765 (Cat. no. HY-13205) and Val-boroPro (Cat. no. HY-13233A) were obtained from MedChemExpress (Monmouth Junction, NJ, USA). Etoposide (Cat. no. A1971) was obtained from ApexBio (Houston, TX, USA). Streptozocin (Cat. no. S0130) was obtained from Sigma Aldrich (St Louis, MO, USA).

Cell culture and treatments

The immortalized human renal tubule epithelial cells (HK-2 cells) (ATCC®CRL-2190™) were cultured in DMEM/F12 supplemented with 10% FBS and 100 U/mL penicillin and streptomycin (Gibco) at 37°C in a humidified 5% CO₂ incubator. HK-2 cells were cultured for 48 h in medium containing 25 mM glucose with or without VX-765 (30 μ M) or Z-YVAD-FMK (10 μ M)^{10,14,15}. In some experiments, the cells were treated with DMSO, Val-boroPro (5 μ M) or etoposide (25 μ M)

for 24 h. The culture supernatants and cells were collected at the indicated times for analysis.

Knockdown of NLRC4 was performed by transfection of siRNA (Sequence 1: CGGGATTTTCAGCAAGTTGAAT and Sequence 2: CACAATCAGGAAGCAGACATT). Non-target siRNA or NLRC4 siRNA were transfected with jetPRIME (PolyPlus) according to the manufacturer's protocol.

Co-immunoprecipitation and immunoblotting

Cells and renal cortices were lysed in RIPA buffer containing protease inhibitors. Protein lysates were fractionated by SDS-polyacrylamide gel electrophoresis and then transferred onto PVDF membrane (Millipore, Billerica, MA, USA). The blots were probed with the appropriate antibodies. The immunocomplex was visualized with Immobilon Western Chemiluminescent HRP Substrate (Millipore) using the ChemiDoc™ Touch Imaging System (Bio-Rad, Hercules, CA, USA). For co-immunoprecipitation assay. We used the rabbit polyclonal anti-NLRC4 antibody as the bait protein to immunoprecipitate antigen, then detected caspase-1. Rabbit IgG was used as a negative control.

Imaging of cell death by microscopy

To examine cell death morphology, HK-2 cells were treated with Val-boroPro or etoposide for 24 h, or high glucose for 48 h. Static microscopic images were captured using DMI3000B Leica Microsystems. The data shown are representative of four randomly selected fields.

Confocal microscopy

HK-2 cells were seeded on 35 mm cover glass-bottom culture dishes. After culturing in high glucose conditions for 48 h, the cells were incubated with the active caspase-1 probe FAM-YVAD-FMK (FLICA) (ImmunoChemistry Technologies, Bloomington, MN, USA). Washing cells with wash buffer before propidium iodide (PI) and Hoechst were added and incubated for 10 min in the dark. The stained live cells were imaged in a Nikon C2 confocal microscope. There were four groups of cells: (i) live cells were defined as FLICA⁻/PI⁻; (ii) caspase-1-activated cells were defined as FLICA⁺/PI⁻; (iii) pyroptotic cells were defined as FLICA⁺/PI⁺¹⁶.

Flow cytometry

After various treatments and transduction, samples were stained with FAM-YVAD-FMK (FLICA) and PI according to the manufacturer's protocol. In order to quantify the percentage of pyroptotic cells, Accuri™ C6 Plus (BD Biosciences, San Jose, CA, USA) was applied to analyze 2000–5000 cells in each experiment approximately. For caspase-1 activation, the cells were incubated with FLICA alone.

Secretion of IL-1 β

The level of IL-1 β in renal cortex homogenate was measured using the mouse interleukin 1 β enzyme-linked immunosorbent

assay kit (CUSABIO, CN) following the manufacturer's instructions. After various treatments, cell culture medium was collected, and the IL-1 β level was quantified by the human IL-1 β ELISA kit (eBioscience, San Diego, CA, USA).

Release of lactate dehydrogenase

Lactate dehydrogenase (LDH) release has been perceived as a hallmark of pyroptosis. CytoTox 96 Cytotoxicity Assay (Promega, Madison, WI, USA) was used to detect LDH activity in the supernatants after the indicated treatments. The activity of released LDH is expressed as a proportion of the total LDH in the cell lysate.

Animal models

Eight-week-old male CD1 (ICR) mice were injected intraperitoneally with 55 mg/kg streptozotocin or 0.1 mol/L citrate buffer (vehicle) for 5 days^{17–19}. 14 days after injection, mice with blood glucose level over 300 mg/dL were considered diabetic^{4,20}. ACCU-CHEK glucose strips were used to detect blood glucose level via tail vein. For the administration of the caspase-1 inhibitor, diabetic mice were administered intraperitoneally with 100 mg/kg VX-765 daily^{12,21} or 20% Cremophor EL (vehicle) for 8 weeks. The treatment with VX-765 was initiated 2 weeks after STZ injection. All experiments with mice were approved by the Laboratory Animal Welfare and Ethics Committee of China Medical University and was performed in conformity to the Guide for the Care and Use of Laboratory Animals.

Blood and urine examination

Blood samples were collected from experimental mice after anesthesia. Urine samples were collected every 2 or 3 weeks. Serum samples were detected for albumin by a standard chemical method. Serum and urine creatinine level as well as serum creatinine and blood urea nitrogen (BUN) level were measured by enzymatic method with commercial kits. The mouse albumin ELISA kit (Abcam) was used to detect urine albumin. All measurements were performed in triplicate.

Histological and immunohistochemical staining

Kidneys from mice undergoing various treatments were fixed in 4% paraformaldehyde, dehydrated in a graded series of ethanol, embedded in paraffin, sectioned (5 μ m), and mounted on glass slides. Paraffin-embedded slices were deparaffinized, rehydrated, and subjected to hematoxylin-eosin (HE) and Masson trichrome staining. Leica DMI4000 B was used to capture images. Tubulointerstitial injury was scored as follows: 0, no damage; 1, <25%; 2, 25–50%; 3, 50–75%; and 4, >75%.

After deparaffinization and rehydration, paraffin-embedded slices were immersed in citrate buffer solution for microwave antigen retrieval, then 3% hydrogen peroxide solution for inactivating peroxidase, followed by 3% BSA for blocking nonspecific binding. The sections were stained with antibodies against

GSDMD, CD45, F4/80 or fibronectin overnight, then further incubated with peroxidase-conjugated secondary antibodies for 1 h. At last, the slides were developed using DAB substrate.

Statistics

Statistical analyses were conducted with Student's *t*-test. ANOVA and Bonferroni *t* tests were performed for the comparison of multiple groups. Paired samples *t*-test was used for two matched-group comparisons. Nonparametric test was conducted using the Kruskal–Wallis test and Mann–Whitney *U* test. Data were considered statistically significant at *P* < 0.05.

RESULTS

High glucose treatment induces NLRC4, caspase-1 and GSDMD activation in renal tubular cells

To determine the role of pyroptosis in renal tubular cells in diabetic nephropathy, we utilized HK-2 cells. The major pathway mediating pyroptosis involves the inflammasome, including an executioner caspase, which is typically caspase-1^{9,22}. We treated HK-2 cells with 5.5, 15, 25, or 35 mM D-glucose or mannitol and found that NLRC4, cleaved caspase-1 and GSDMD p30 fragment increased with glucose concentrations (Figure 1a, b). To clarify whether caspase-1 is activated in HK-2 cells through an NLRC4-dependent mechanism, we conducted an immunoprecipitation assay and NLRC4 knockdown and found that NLRC4 bound to caspase-1 (Figure 1c) and regulated the cleavage of caspase-1 (Figure 1d, e). These observations demonstrate that the NLRC4 inflammasome is involved in the activation of inflammatory caspase-1, a previously unrecognized mechanism in glucose-stressed HK-2 cells.

High glucose treatment induces caspase-1-mediated pyroptosis in renal tubular cells

Pyroptosis, unlike apoptosis, is characterized by membrane pore formation, swelling, and typically membrane ballooning^{23,24}. First, we imaged cells exposed to high glucose, Val-boroPro or etoposide. It has been demonstrated that Val-boroPro mediates pyroptosis via activating pro-caspase-1²⁵, while etoposide induces apoptosis²⁶. Consistent with these reports, Val-boroPro treatment in HK-2 cells activated inflammatory caspase-1, while etoposide markedly induced apoptotic caspase-3 cleavage (Figure 2a). As shown in Figure 2b, high glucose-induced cell death exhibited pyroptotic-like morphological feature, membrane ballooning, closely resembling Val-boroPro-treated cells. As pyroptosis is a lytic form of cell death mediated by caspase-1, FLICA⁺/PI⁺ cells were defined as pyroptosis. With confocal microscopy, pyroptotic cells were observed to exhibit membrane ballooning (Figure 2c), further confirming the development of pyroptosis in glucose-stressed HK-2 cells. In addition, as shown in Figure 2d and e, pyroptosis was promoted in glucose-stressed cells as assessed by fluorescence microscopy. Consistently, flow cytometry analysis showed that glucose induced an increased population of pyroptosis, with a more significant effect after 48 h of treatment. While osmotic pressure

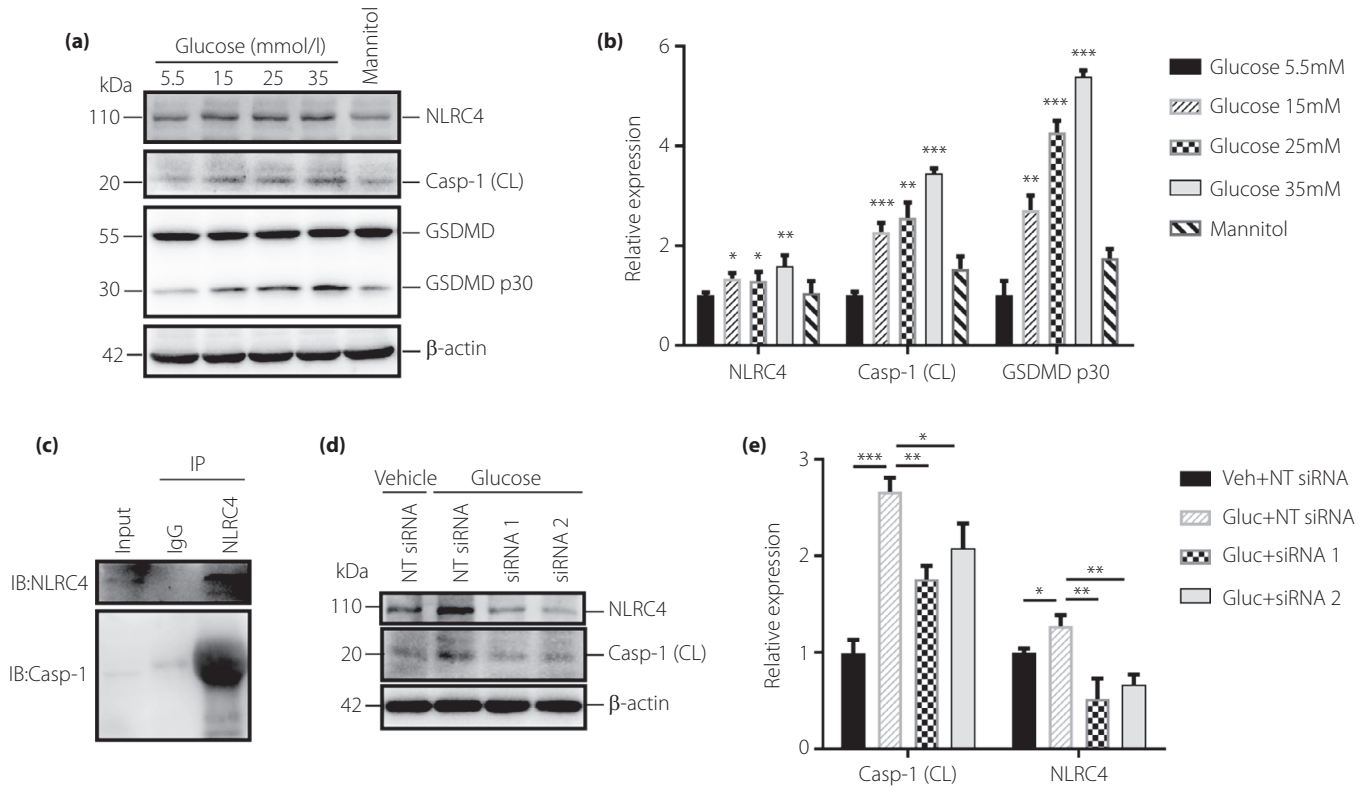


Figure 1 | High glucose activates NLRC4, caspase-1 and GSDMD in HK-2 cells. (a) Effects of the indicated concentrations of glucose or mannitol (5.5 mM glucose+29.5 mM mannitol) on inflammasome and GSDMD activation were evaluated by immunoblotting. Densitometry analysis of the data in (b). (c) Immunoprecipitation assay of high glucose-treated cells. Lysates were immunoprecipitated with anti-NLRC4 antibody. Caspase-1 was analyzed by immunoblotting. (d and e) Knocking down NLRC4 using siRNA transfection downregulated cleaved caspase-1 protein levels. Densitometry analysis of the data in e. Data are presented as mean \pm SEM. Results represent at least three independent experiments. CL, cleaved; Etop, etoposide; FL, full length; Gluc, glucose; NT siRNA, non-target siRNA; VbP, Val-boroPro; Veh, vehicle. * P < 0.05; ** P < 0.01; *** P < 0.001, ANOVA and Bonferroni t tests were performed.

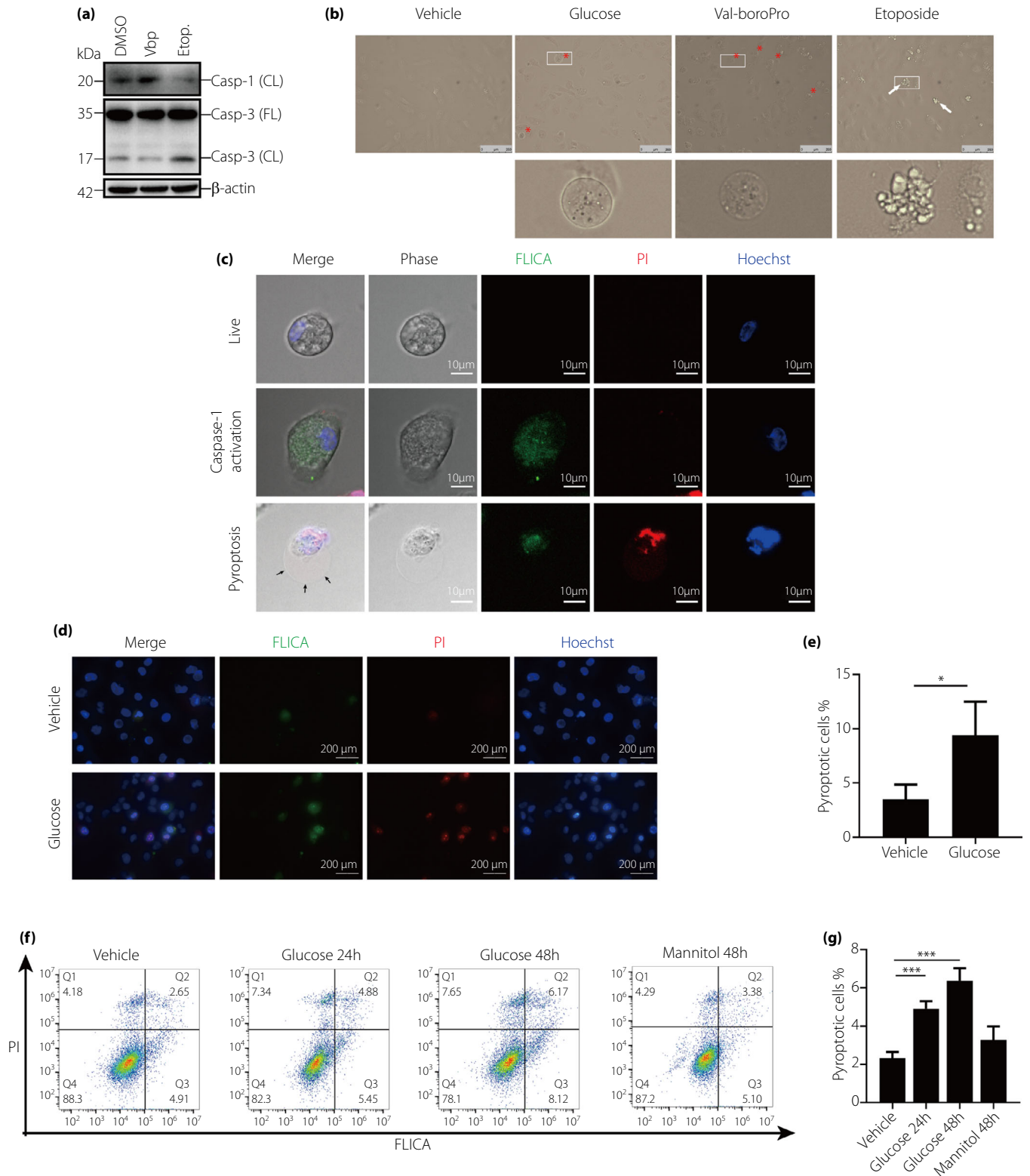
caused by mannitol was not the main factor inducing pyroptosis (Figure 2f, g). Collectively, treatment of HK-2 cells with high glucose induces pyroptosis.

Caspase-1 mediates pyroptosis and inflammatory signaling in glucose-stressed tubular cells

To confirm that caspase-1 is essential for high glucose-induced pyroptosis in HK-2 cells, the cells were pretreated with the

selective caspase-1 inhibitors VX-765 or Z-YVAD-FMK for 30 min. We detected caspase-1 activity using the FLICA-labeled YVAD probe and found that both VX-765 and Z-YVAD-FMK inhibited upregulated caspase-1 activity in high glucose (Figure 3a, b). Caspase-1 inhibitor treatments prevented the increased GSDMD p30 fragment and mature IL-1 β expression in glucose-stressed HK-2 cells. As expected, upregulated NLRC4 was not affected (Figure 3c, e). Besides, noncanonical

Figure 2 | High glucose promotes pyroptosis in HK-2 cells. (a) Immunoblots of HK-2 cells treated with 5 μ M Val-boroPro, 25 μ M etoposide or DMSO for 24 h. (b) Observations of HK-2 cells treated with Val-boroPro, etoposide or 25 mM D-glucose for 48 h by microscope. Asterisks indicate ballooning pyroptotic cells. Arrows indicate blebbing apoptotic cells. Scale bar = 250 μ m. The illustration shows magnification of the area shown by the white line. (c) Glucose-stressed cells stained with FLICA (green), PI (red) and Hoechst (blue) in confocal microscopy. The first panel shows normal cells (PI $^-$ and FLICA $^-$), the second panel shows caspase-1-activated cells (PI $^-$ and FLICA $^+$), and the third panel shows pyroptotic cells (PI $^+$ and FLICA $^+$). Arrows indicate ballooning pyroptotic cell. Scale bar = 10 μ m. (d) Cells in response to control (vehicle) or high glucose treatment under a fluorescence microscope. Graph summarizing the ratio of FLICA $^+$ /PI $^+$ cells in (e). Scale bar = 200 μ m. (f and g) Flow cytometry analysis of cells treated with 25 mM glucose or mannitol for 24 or 48 h. PI $^+$ and FLICA $^+$ cells in quadrant 2 are pyroptotic cells. Data are presented as mean \pm SEM. Results represent at least three independent experiments. *** P < 0.001, Student's t -test for panel e and ANOVA and Bonferroni t tests for panel g.



pyroptosis mediated by caspase-4 and -5 (caspase-11 in mice) also occurs in various cell types^{27,28}, but is still undefined in DN. Our results showed that cleaved caspase-4 and caspase-5

levels were comparable between these groups, excluding their participation in high glucose-mediated damage to tubular cells (Figure 3d). Pyroptosis involves membrane pore formation,

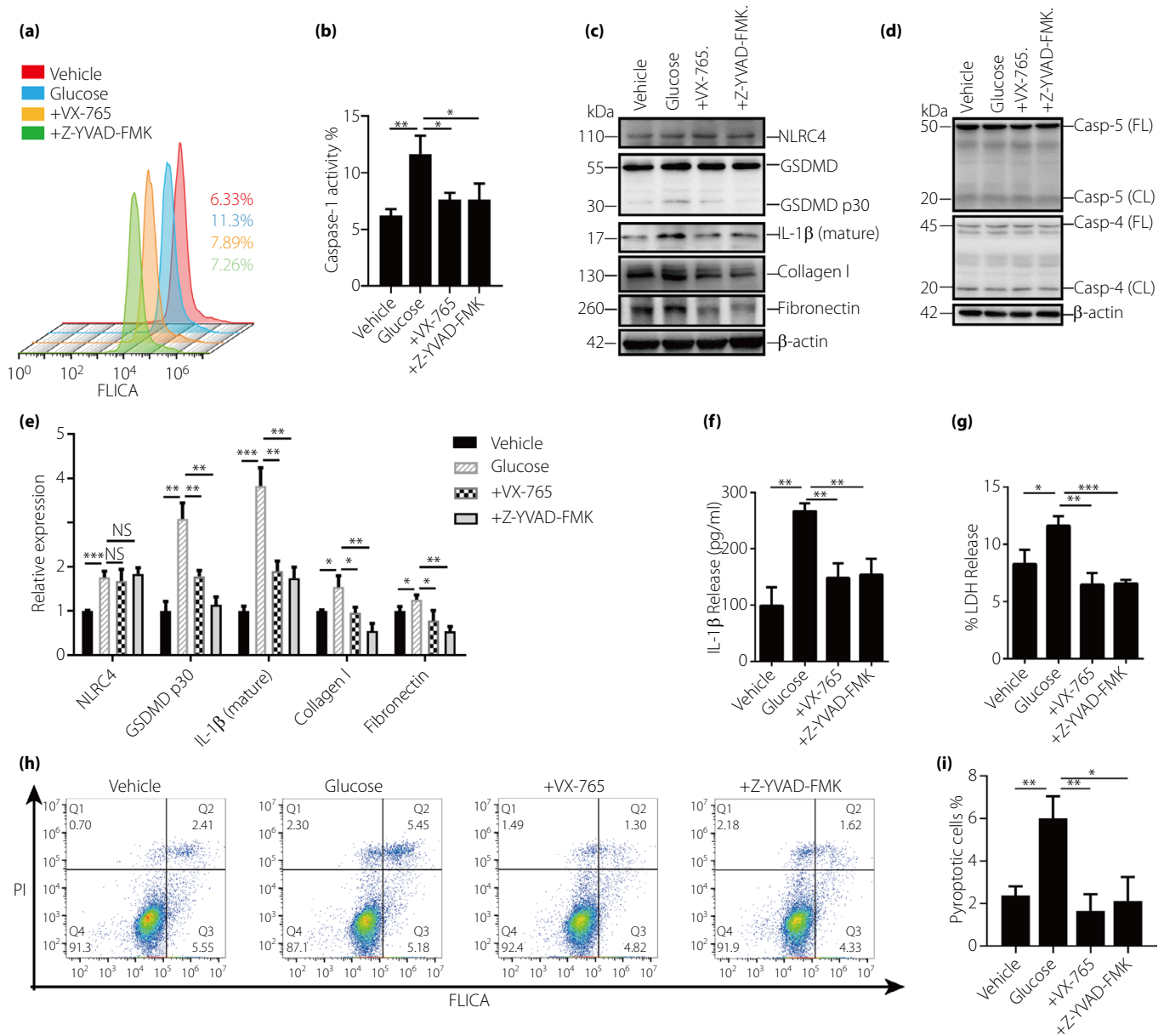


Figure 3 | High glucose-induced pyroptosis in HK-2 cells was blocked by caspase-1 inhibitors. (a and b) Treatment with either VX-765 or Z-YVAD-FMK before and during high glucose exposure inhibited caspase-1 activity in renal tubular cells, as assessed by flow cytometry after FLICA staining. (c) Immunoblots were probed with anti-NLRC4, anti-GSDMD, anti-IL-1β, anti-collagen I or anti-fibronectin antibodies. Densitometry analysis of the data in (e). (d) The blots showing the expression of cleaved caspase-4 and caspase-5. (f) Graph represents the level of IL-1β in the supernatant, as examined by ELISA. (g) Cell death was measured by LDH release. (h) Flow cytometry analysis shows that incubation with VX-765 or Z-YVAD-FMK reduced pyroptosis in glucose-stressed HK-2 cells. Graph summarizing the ratio of pyroptotic cells in (i). Data are presented as mean ± SEM. Results represent at least three independent experiments. CL, cleaved; FL, full length; IL, interleukin. **P* < 0.05; ***P* < 0.01; ****P* < 0.001, ANOVA and Bonferroni *t* tests were performed.

ultimately resulting in the release of cytokines and cytosolic contents^{29,30}. Enzyme-linked immunosorbent assay revealed that inhibiting caspase-1 decreased IL-1β released into the medium in high glucose (Figure 3f). Pyroptosis was also evaluated by assaying LDH release. Caspase-1 inhibition reduced LDH release from glucose-stressed tubular cells (Figure 3g). Flow

cytometry analysis revealed that treatment with VX-765 or Z-YVAD-FMK reduced pyroptosis in high glucose (Figure 3h, i). Moreover, caspase-1 inhibition strikingly decreased collagen I and fibronectin expression (Figure 3c, e). These results suggest that caspase-1 is important in the regulation of pyroptosis and cell survival in high glucose-stressed tubular cells.

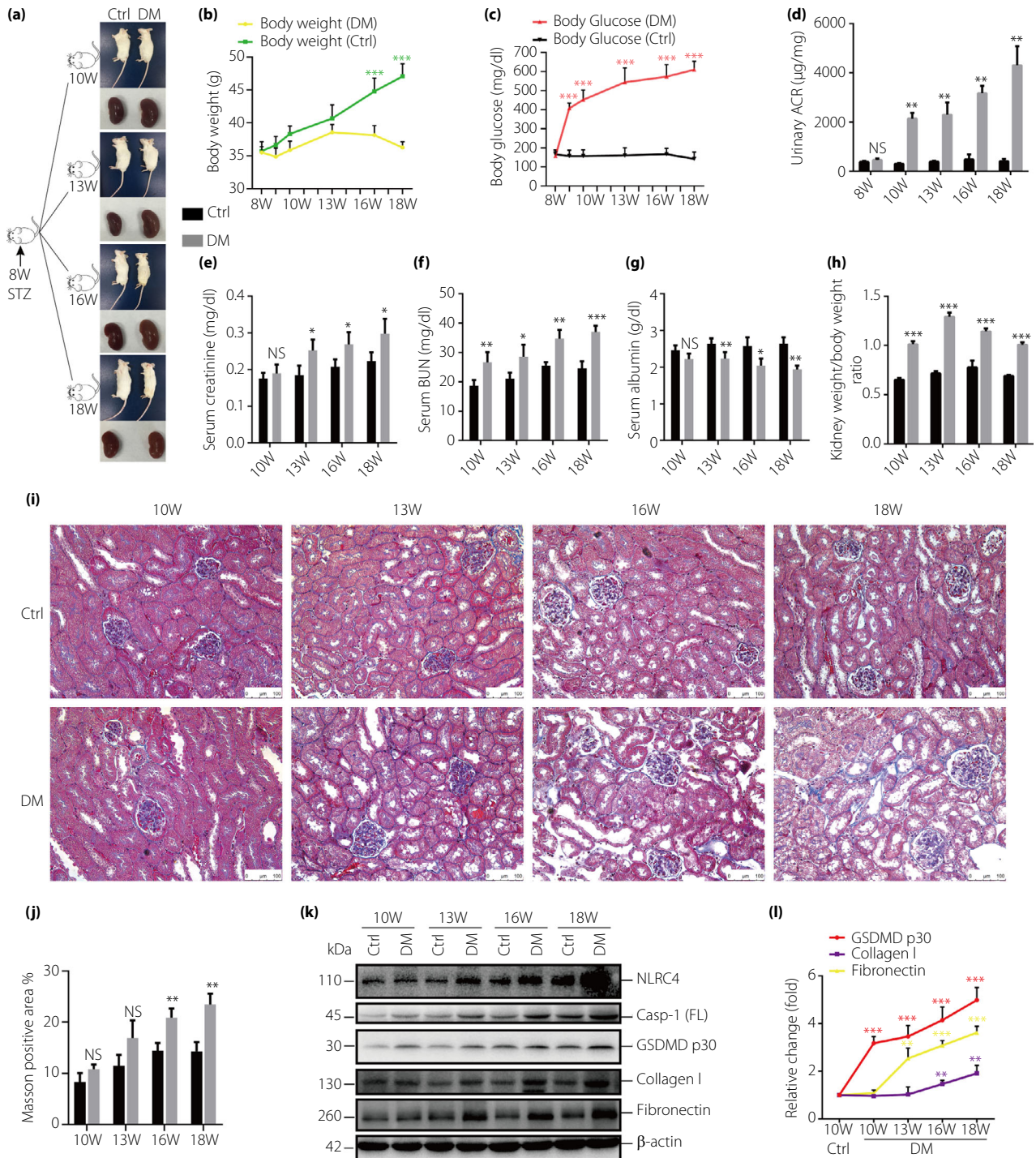
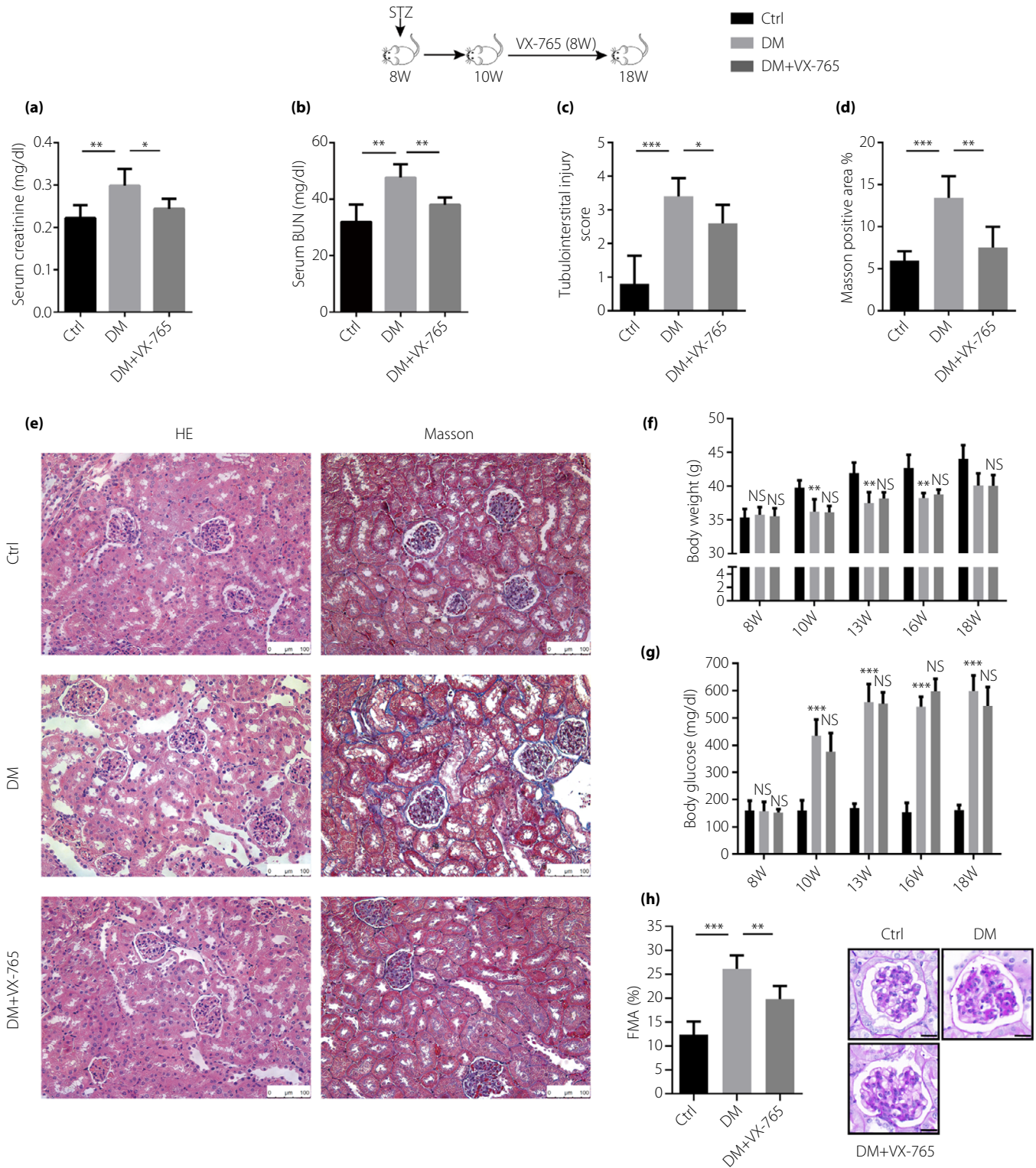


Figure 4 | Caspase-1-mediated pyroptosis is associated with the onset of DN. (a) Representative images of kidney volume differences between nondiabetic (Ctrl) and diabetic (DM) mice of different ages. Body weights (b) and blood glucose levels (c) and of mice. Albuminuria (d), serum creatinine (e), BUN (f) and serum albumin (g) levels of mice. (h) Kidney/body weight ratio of mice at different ages. (i) Masson staining to determine the extent of tubulointerstitial fibrosis. Figure presenting results of determining the blue staining area in (j). (k) Immunoblots of NLRC4, caspase-1, GSDMD p30, collagen I and fibronectin in renal cortex extracts from mice of different ages. Densitometry analysis of GSDMD p30, collagen I and fibronectin in (l). Data are presented as mean ± SEM. *n* = 5–7. Scale bar = 100 µm. ACR, albumin-to-creatinine ratio; Ctrl, control; DM, diabetic mice; FL, full length; NS, not significant; STZ, streptozocin; W, week-old. **P* < 0.05; ***P* < 0.01; ****P* < 0.001 for diabetic mice versus nondiabetic mice. Paired samples *t*-test for panel b, c, e, f, g and j, Kruskal–Wallis test and Mann–Whitney test for panel d and h, and ANOVA and Bonferroni *t* tests for panel l.



The onset of diabetic nephropathy is associated with caspase-1-mediated pyroptosis

Diabetes was induced in 8-week-old male CD-1 mice by streptozotocin (STZ) injection for five consecutive days (55 mg/kg

intraperitoneally). These mice developed stable hyperglycemia levels within 7 days (Figure 4c). The kidney/body weight ratio of diabetic mice was notably greater than that of nondiabetic mice and peaked at the age of 13 weeks, confirming the state of

Figure 5 | VX-765 protects against renal injury in diabetic mice. (a) Serum creatinine, (b) BUN levels of nondiabetic mice (Ctrl), diabetic mice (DM), and diabetic mice treated with VX-765 (DM+VX-765). (c) Hematoxylin-eosin and Masson staining of representative kidney slices indicated alleviated tubular injury and tubulointerstitial fibrosis with the administration of VX-765 in diabetic mice. Semiquantitative analysis of tubular injury in (c). Figure presenting results of determining the blue staining area in (d). Body weight (f) and blood glucose (g) of control, DM and DM+VX-765 group mice at different ages. (h) Fractional mesangial area (FMA) was decreased in VX-765-treated diabetic mice as compared with diabetic mice. Data are presented as mean \pm SEM. $n = 5-7$. Scale bar = 100 μm , scale bar = 20 μm for (h). NS, not significant. * $P < 0.05$; ** $P < 0.01$; *** $P < 0.001$, ANOVA and Bonferroni t tests were performed.

hyperfiltration and hyperperfusion (Figure 4a, h). Albuminuria, BUN levels in diabetic mice increased with age (Figure 4d–g). Histopathological analysis demonstrated that 16- and 18-week-old diabetic mice showed progressive renal fibrosis (Figure 4i, j).

To clarify the relevance of caspase-1 in diabetic nephropathy, we analyzed the kinetic processes of inflammation and fibrosis in diabetic mice. Immunoblot analyses showed that NLRC4 and caspase-1 expression initially increased in the renal cortex of 10-week-old diabetic mice, compared with that in the control. Consistent with caspase-1 expression, pyroptotic indicator GSDMD p30 was also increased in 10-week-old diabetic mice. Thus, inflammasome activation and pyroptosis occur at an early stage of DN. Fibronectin and collagen I were significantly increased in 13- or 16-week-old diabetic mice, suggesting that caspase-1-mediated pyroptosis precedes and is potentially linked with renal fibrosis in DN (Figure 4k, l).

VX-765 administration protects mice from diabetic nephropathy

To further confirm the role of caspase-1 in the development of DN and investigate whether the caspase-1 inhibitor VX-765 is an effective therapeutic approach for diabetic nephropathy, diabetic mice were administered with 100 mg/kg VX-765 for 8 weeks. Administration of VX-765 in diabetic mice effectively ameliorated renal function, compared with that of untreated diabetic mice (Figure 5a, b). Histological features were determined by HE and Masson trichrome in diabetic mice and revealed that renal injury and fibrosis were amendable to caspase-1 inhibition (Figure 5c–e). VX-765 treatment did not affect blood glucose level or body weight (Figure 5f, g), illustrating that VX-765 ameliorated diabetic nephropathy independent of its metabolic effects.

VX-765 administration ameliorates renal inflammation in diabetic mice

In vitro, our results demonstrated that VX-765 effectively regulated pyroptosis and inflammation of tubular cells in high glucose by inhibiting caspase-1 activity. As expected, there was marked inhibition of the pyroptotic indicators GSDMD p30 and mature IL-1 β expression in VX-765-treated diabetic mice relative to those in untreated diabetic mice (Figure 6A, B). The IL-1 β level was also decreased in renal cortex homogenate following VX-765 treatment, as assessed by ELISA (Figure 6C). Furthermore, immunohistochemistry revealed increased positivity for GSDMD at the tubular level in diabetic mice and mild

staining of GSDMD in podocytes. These changes were significantly attenuated in VX-765-treated mice (Figure 6D, Ha–d). Immunohistochemical analysis of CD45 or F4/80 expression indicated inflammatory cell infiltration in the kidney of diabetic mice, whereas the number of CD45+ or F4/80+ cells was reduced after VX-765 administration (Figure 6E, F, He–l). Additionally, immunoblot (Figure 6A, B) and immunological staining (Figure 6G, Hm–p) of fibrosis indicators also showed that the upregulated collagen I and fibronectin deposition in diabetic mice were markedly blunted after treatment with VX-765. Overall, this work suggests that administration of VX-765 can slow the progression of diabetic nephropathy in mice through prevention of caspase-1-mediated pyroptosis and renal inflammation.

DISCUSSION

Researchers have reported that hyperglycemia induced pyroptosis in diabetic cardiomyopathy³¹. Moreover, several recent studies have confirmed that tubular epithelial pyroptosis is a vital pathogenesis of renal ischemia/reperfusion injury and contrast-mediated acute kidney injury^{32,33}, suggesting that pyroptosis has a crucial role in tubular injury. Pyroptosis has not been unequivocally described in diabetic nephropathy, although signs of inflammasome activation have been observed in the initiation and progress of DN. In our study, characteristic morphological and biochemical features of pyroptosis were observed in glucose-stressed tubular cells, including GSDMD cleavage, ballooned cell membrane accompanied with caspase-1 immunoreactivity, release of proinflammatory cytokines, and release of cellular contents. Pyroptotic cells further amplify renal damage through the release of inflammatory mediators (e.g., cytokines) and damage-associated molecular patterns (DAMPs). These components drive a persistent inflammatory cascade which activates infiltrating leukocytes^{34,35}. Therefore, therapies targeting tubular pyroptosis might exert renoprotective effects by preventing cytotoxic molecules release.

In vitro, we confirmed that caspase-1 inhibitors effectively regulate the occurrence of pyroptosis in tubular cells in high glucose. Indeed, caspase-1 inhibition may be superior to blockade of inflammasome, as caspase-1 is the common component of canonical inflammasomes. Recent research showed that treatment of experimental autoimmune encephalomyelitis animals with VX-765 diminished the expression of inflammation-associated proteins in central nervous system, and mitigated

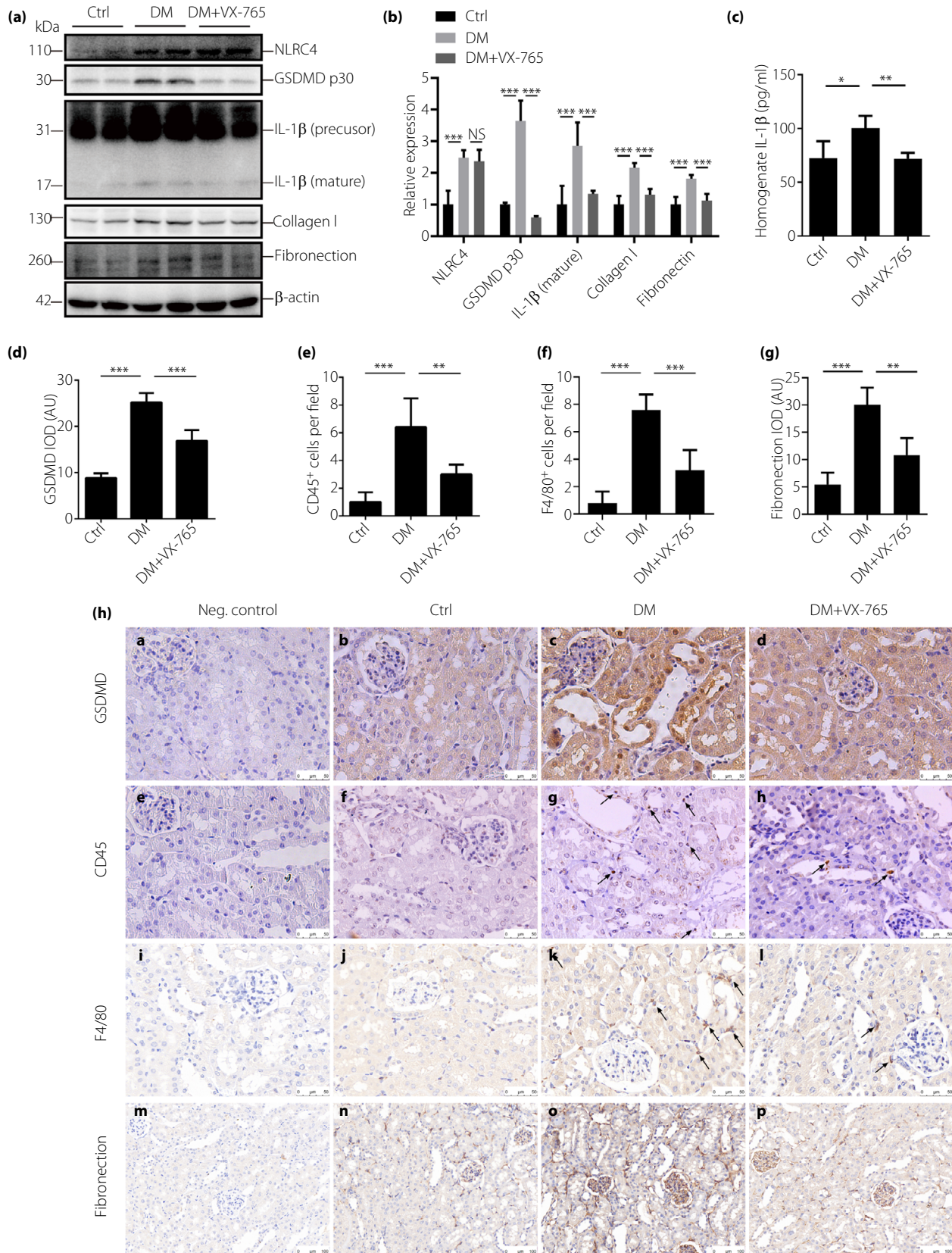


Figure 6 | VX-765 ameliorates inflammation and fibrosis in diabetic mice. (A) Immunoblotting of renal cortex extracts from nondiabetic mice (Ctrl), diabetic mice (DM) and diabetic mice treated with VX-765 (DM+VX-765). Densitometry analysis of the data in (B). (C) IL-1 β level in renal cortex homogenate of mice determined by ELISA. (H) Images showing immunohistochemical staining with anti-GSDMD (a–d), anti-CD45 (e–h), anti-F4/80 (i–l) and anti-fibronectin (m–p) antibodies in the indicated groups. Negative control using a non-specific primary antibody (Neg. control). Arrows indicate CD45+ or F4/80+ cells. Graphs summarizing the integrated optical density (IOD) data in (D, G). Data are presented as mean \pm SEM. Scale bar = 50 μ m, scale bar = 100 μ m for fibronectin. AU, arbitrary units; IL, interleukin; Neg. control, negative control; NS, not significant. ****P** < 0.01; *****P** < 0.001, ANOVA and Bonferroni *t* tests were performed.

axonal damage³⁴. Audia *et al.*¹⁵ first demonstrated that administration of VX-765 at reperfusion provides myocardial infarct size reduction and preservation of ventricular function. In the present study, we demonstrate that VX-765 ameliorated renal dysfunction, tubular injury, and renal inflammation in mice with DN, but had no effect on blood glucose level or body weight, illustrating that VX-765 represents a novel and efficacious therapeutic treatment for DN without increasing the risk of hypoglycemia in diabetic patients.

The upstream sensors for caspase-1 activation differ depending on different cellular states and ligands including NLRP3, NLRC4, NLRP1, pyrin and AIM2³⁶. NLRP3 is the best studied inflammasome activating caspase-1^{37,38}. However, the role of other inflammasomes in DN remains poorly defined. Our research surprisingly found that the NLRC4 is involved in DN and in the activation of caspase-1 in glucose-stressed HK-2 cells. While the mechanism underlying NLRC4 activation in renal resident cells still requires further investigation, as NLRC4 inflammasome in macrophages is mainly activated by flagellin and the type III secretion system^{22,39}.

The STZ-dependent model of type 1 diabetes, may have limitations, and that db/db mice with obesity or insulin resistance might be preferred. However, hyperglycemia itself is enough to trigger inflammasome activation. A previous study also showed that renoprotection by inflammasome inhibition is independent of these metabolic factors^{4,40}. In addition, ICR mice injected with STZ develop fibrosis within 8–10 weeks without the need for uninephrectomy, hence allowing for rapid analyses of the effects of therapeutic interventions. Therefore, we believe that the method chosen is a reasonable approach.

In summary, this report provides compelling molecular and morphological evidence for tubular pyroptosis in high glucose conditions. We also demonstrated that caspase-1 effectively regulates pyroptosis and fibrosis in diabetic nephropathy. Administration of VX-765 to diabetic animals ameliorated renal function, inflammation and fibrosis.

ACKNOWLEDGMENTS

This work was supported by grants from the Chinese National Key Technology R and D Program, Ministry of Science and Technology (No. 2017YFC0907601, 2017YFC0907602, 2017YFC0807603), Natural Science Foundation of China (No. 81770724, 81800642), Shenyang Science and Technology Bureau (No. RC170172), Doctoral Scientific Research Foundation of Liaoning Province (20180540113).

DISCLOSURE

The authors declare no conflict of interest.

Approval of the research protocol: All experiments with mice were approved by the Laboratory Animal Welfare and Ethics Committee of China Medical University.

Informed consent: N/A.

Approval date of Registry and the Registration No. of the study/trial: The study was approved on March 18, 2019 (IACUC Issue No. CMU2019179).

Animal studies: All animal experiments were conducted following the national guidelines and the relevant national laws on the protection of animals.

REFERENCES

- Gilbert RE. Proximal tubulopathy: prime mover and key therapeutic target in diabetic kidney disease. *Diabetes* 2017; 66: 791–800.
- He X, Cheng R, Park K, *et al.* Pigment epithelium-derived factor, a noninhibitory serine protease inhibitor, is renoprotective by inhibiting the Wnt pathway. *Kidney Int* 2017; 91: 642–657.
- Winter L, Wong LA, Jerums G, *et al.* Use of readily accessible inflammatory markers to predict diabetic kidney disease. *Front Endocrinol (Lausanne)* 2018; 9: 225.
- Shahzad K, Bock F, Dong W, *et al.* Nlrp3-inflammasome activation in non-myeloid-derived cells aggravates diabetic nephropathy. *Kidney Int* 2015; 87: 74–84.
- Yiu WH, Wong DW, Wu HJ, *et al.* Kallistatin protects against diabetic nephropathy in db/db mice by suppressing AGE-RAGE-induced oxidative stress. *Kidney Int* 2016; 89: 386–398.
- Rathkey JK, Zhao J, Liu Z, *et al.* Chemical disruption of the pyroptotic pore-forming protein gasdermin D inhibits inflammatory cell death and sepsis. *Sci Immunol* 2018; 3: eaat2738.
- Ding J, Wang K, Liu W, *et al.* Pore-forming activity and structural autoinhibition of the gasdermin family. *Nature* 2016; 535: 111–116.
- Xia S, Hollingsworth LR, Wu H. Mechanism and regulation of gasdermin-mediated cell death. *Cold Spring Harb Perspect Biol* 2020; 12: a036400.
- Orning P, Lien E, Fitzgerald KA. Gasdermins and their role in immunity and inflammation. *J Exp Med* 2019; 216: 2453–2465.
- Flores J, Noel A. Caspase-1 inhibition alleviates cognitive impairment and neuropathology in an Alzheimer's disease mouse model. *Nat Commun* 2018; 9: 3916.

11. Incorporated VP. Vertex Announces Completion of Phase 2 Study of VX-765 in People with Epilepsy who did not Respond to Previous Treatment. Available from: <https://investorsVRTX.com/static-files/99195d36-42be-4e2a-a2b3-b0d632ba31c7>. Accessed March 10, 2011.
12. Bassil F, Fernagut PO, Bezdard E, et al. Reducing C-terminal truncation mitigates synucleinopathy and neurodegeneration in a transgenic model of multiple system atrophy. *Proc Natl Acad Sci USA* 2016; 113: 9593–9598.
13. Shahzad K, Bock F, Al-Dabet MM, et al. Caspase-1, but not caspase-3, promotes diabetic nephropathy. *J Am Soc Nephrol* 2016; 27: 2270–2275.
14. Ding HG, Deng YY, Yang RQ, et al. Hypercapnia induces IL-1beta overproduction via activation of NLRP3 inflammasome: implication in cognitive impairment in hypoxemic adult rats. *J Neuroinflammation* 2018; 15: 4.
15. Audia JP, Yang XM, Crockett ES, et al. Caspase-1 inhibition by VX-765 administered at reperfusion in P2Y12 receptor antagonist-treated rats provides long-term reduction in myocardial infarct size and preservation of ventricular function. *Basic Res Cardiol* 2018; 113: 32.
16. Alfonso-Loeches S, Urena-Peralta JR, Morillo-Bargues MJ, et al. Role of mitochondria ROS generation in ethanol-induced NLRP3 inflammasome activation and cell death in astroglial cells. *Front Cell Neurosci* 2014;8:216.
17. Zhan M, Usman IM, Sun L, et al. Disruption of renal tubular mitochondrial quality control by Myo-inositol oxygenase in diabetic kidney disease. *J Am Soc Nephrol* 2015; 26: 1304–1321.
18. Lee HA, Lee JH, Han JS. A phlorotannin constituent of *Ecklonia cava* alleviates postprandial hyperglycemia in diabetic mice. *Pharm Biol* 2017; 55: 1149–1154.
19. Reddy S, Chang M, Robinson E. Young NOD mice show increased diabetes sensitivity to low doses of streptozotocin. *Ann N Y Acad Sci* 2006; 1079: 109–113.
20. Isermann B, Vinnikov IA, Madhusudhan T, et al. Activated protein C protects against diabetic nephropathy by inhibiting endothelial and podocyte apoptosis. *Nat Med* 2007; 13: 1349–1358.
21. Maroso M, Balosso S, Ravizza T, et al. Interleukin-1beta biosynthesis inhibition reduces acute seizures and drug resistant chronic epileptic activity in mice. *Neurotherapeutics* 2011; 8: 304–315.
22. Xue Y, Enosi Tuipulotu D, Tan WH, et al. Emerging activators and regulators of inflammasomes and pyroptosis. *Trends Immunol* 2019; 40: 1035–1052.
23. Lu H, Zhang S, Wu J, et al. Molecular targeted therapies elicit concurrent apoptotic and gsdme-dependent pyroptotic tumor cell death. *Clin Cancer Res* 2018; 24: 6066–6077.
24. Chen KW, Demarco B, Heilig R, et al. Extrinsic and intrinsic apoptosis activate pannexin-1 to drive NLRP3 inflammasome assembly. *EMBO J* 2019; 38: e101638.
25. Okondo MC, Johnson DC, Sridharan R, et al. DPP8 and DPP9 inhibition induces pro-caspase-1-dependent monocyte and macrophage pyroptosis. *Nat Chem Biol* 2017; 13: 46–53.
26. Taabazuing CY, Okondo MC, Bachovchin DA. Pyroptosis and apoptosis pathways engage in bidirectional crosstalk in monocytes and macrophages. *Cell Chem Biol* 2017; 24: 507–14 e4.
27. Kayagaki N, Warming S, Lamkanfi M, et al. Non-canonical inflammasome activation targets caspase-11. *Nature* 2011; 479: 117–121.
28. Shi J, Zhao Y, Wang Y, et al. Inflammatory caspases are innate immune receptors for intracellular LPS. *Nature* 2014; 514: 187–192.
29. Liu X, Zhang Z, Ruan J, et al. Inflammasome-activated gasdermin D causes pyroptosis by forming membrane pores. *Nature* 2016; 535: 153–158.
30. Shi J, Zhao Y, Wang K, et al. Cleavage of GSDMD by inflammatory caspases determines pyroptotic cell death. *Nature* 2015; 526: 660–665.
31. Li X, Du N, Zhang Q, et al. MicroRNA-30d regulates cardiomyocyte pyroptosis by directly targeting foxo3a in diabetic cardiomyopathy. *Cell Death Dis* 2014; 5: e1479.
32. Zhang Z, Shao X, Jiang N, et al. Caspase-11-mediated tubular epithelial pyroptosis underlies contrast-induced acute kidney injury. *Cell Death Dis* 2018; 9: 983.
33. Miao N, Yin F, Xie H, et al. The cleavage of gasdermin D by caspase-11 promotes tubular epithelial cell pyroptosis and urinary IL-18 excretion in acute kidney injury. *Kidney Int* 2019; 96: 1105–1120.
34. McKenzie BA, Mamik MK, Saito LB, et al. Caspase-1 inhibition prevents glial inflammasome activation and pyroptosis in models of multiple sclerosis. *Proc Natl Acad Sci USA* 2018; 115: E6065–E6074.
35. Vande Walle L, Lamkanfi M. Snapshot of a deadly embrace: the Caspase-1-GSDMD interface. *Immunity* 2020; 53: 6–8.
36. Place DE, Kanneganti TD. Cell death-mediated cytokine release and its therapeutic implications. *J Exp Med* 2019; 216: 1474–1486.
37. Qiu YY, Tang LQ. Roles of the NLRP3 inflammasome in the pathogenesis of diabetic nephropathy. *Pharmacol Res* 2016; 114: 251–264.
38. El-Horany HE, Abd-Elatif RN, Watany M, et al. NLRP3 expression and urinary HSP72 in relation to biomarkers of inflammation and oxidative stress in diabetic nephropathy patients. *IUBMB Life* 2017; 69: 623–630.
39. Andrade WA, Zamboni DS. NLR4 biology in immunity and inflammation. *J Leukocyte Biol* 2020; 69: 623–630.
40. Birnbaum Y, Bajaj M, Qian J, et al. Dipeptidyl peptidase-4 inhibition by Saxagliptin prevents inflammation and renal injury by targeting the Nlrp3/ASC inflammasome. *BMJ Open Diabetes Res Care* 2016; 4: e000227.